SPCOLA: JOINT TOPOGRAPHY SOLUTIONS OF BENNU FROM LASER ALTIMETRY AND STEREOPHOTOCLINOMETRY J. H. Roberts[1], O. S. Barnouin[1], R. W. Gaskell[2], E. E. Palmer[2], J. Weirich[2], M. Daly[3], J. Seabrook[3], R. C. Espiritu[1], A. H. Nair[1], and D. Lauretta[4] [1]Johns Hopkins University Applied Physics Laboratory, 11100 Johns Hopkins Rd., Laurel, MD 20723-6099, [2]Planetary Science Institute, 1700 E. Fort Lowell, Tucson, AZ, 85719-2395. [3]York University, 4700 Keele Street, Toronto, ON, Canada, M3J 1P3, [4]Lunar and Planetary Laboratory, University of Arizona, Tucson, AZ. Corresponding Author's Email: James.Roberts@jhuapl.edu

Introduction: Two instruments on OSIRIS-REx enable independent determination of topography. The OSIRIS-REx Camera Suite (OCAMS) returns imaging data. Using stereophotoclinometry (SPC) on these images, we can construct slope and albedo maps or "maplets" of small patches of surface with central control points [1]. The OSIRIS-REx Laser Altimeter (OLA) is a scanning lidar that ranges to the surface, and can be used to develop local and global scale topographic maps. Combining SPC with OLA leverages the strengths of both techniques while mitigating their respective weaknesses, and allows us to generate Digital Elevation Models (DEMs) with higher accuracy than would be possible from either data set alone.

SPC: The strength of SPC is that it provides solutions of topography with accuracies similar to those of the best images used [1–3]. SPC makes use of images at a wide range of viewing geometries, illuminations and resolutions that can fill in gaps where altimetric data from other sources may not exist. SPC also provides precise control point location from large stereo separation over multiple trajectories and even multiple spacecraft. This technique has been used successfully to characterize the topography of several small bodies, including Eros, Phobos, Mimas, Lutetia, Itokawa, Vesta, comet 67P, Mercury and the Moon [4–12].

OLA: Key strengths of lidar ranging include the ability to operate under any illumination conditions, including in the dark and providing absolute measure of the range constraint to the surface. This range can be used to derive a control network for SPC. The range improves the knowledge of the spacecraft position and provides constraints for any gravity solution obtained with radio science. OLA is unique from other altimeters, in that it is capable of firing at 100Hz and 10kHz depending on range from the surface. It also possesses a scanning mirror that can span ±6 degrees. The laser has a 100-200 µrad spot size (depending on range), corresponding to 7 cm spot site in the orbital phase, and an absolute precision of ±3 cm vertically.

SPCOLA Process: Because OSIRIS-REx does not arrive at its target until 2019, we test the SPCOLA technique using synthetic data. A high resolution "truth" model has been generated for this purpose, which has been virtually imaged and scanned. This model has 5 cm global resolution for most regions of the asteroids, and >1 cm resolution near a plausible sample site. The virtual images and scans are generated according to planned trajectory of the real flight system. A series of shape models has been constructed from these synthetic images [13]. We take one of these shape models with the associated 30-cm maplets as an initial framework.

The next step is to process the OLA data into a format compatible with the SPC utilities. We take the synthetic OLA database (including spacecraft navigation errors and instrument noise) for Orbital Phase B [14], and generate a series of 5-cm "mapolas", maps made from the OLA data in the same file format as the SPC maplets. We then use the SPC utilities to bring the mapolas into the existing SPC solution. The spacecraft–surface vector of each mapola is adjusted to minimize the misfit between the mapola and images in the same area, and the initially blank albedo field in the mapola is populated from the SPC solution. At this stage, the mapola solution itself is not altered by SPC, only its position. In this way, we have heights for a given region determined independently by both SPC and OLA. Finally, we generate larger "bigmaps" from

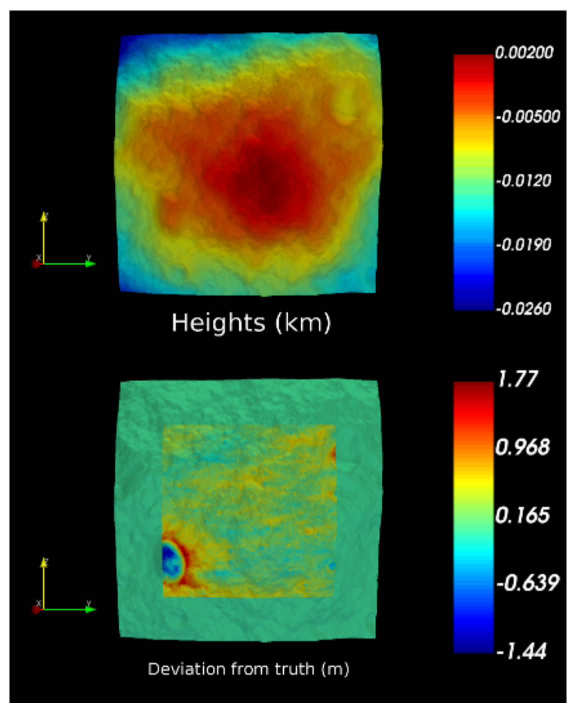

Figure 1: Heights relative to a plane generated from SPC maplets for a 20° by 20° region centered at 0 °N, 10 °E (top) and deviation from truth (bottom).

the mapolas and maplets contained within that region.

Results: In Figure 1, we show a 20° by 20° bigmap (corresponding to 86 m by 86 m on Bennu) of the heights relative to a plane generated from SPC maplets centered at 0 °N, 10 °E (top) and the difference between it and the truth in the central portion of the region (bottom). The SPC solution performs well in most areas, but significantly underestimates the heights of blocks and the depths of craters.

In Figure 2, we show similar bigmaps generated from mapolas. However, we have left some small gaps between mapolas to illustrate the synergy between the data sets. In areas covered by mapolas, the solution matches the truth well, including the boulder. Note that the scale bar on the difference plot is a factor of ~3 smaller than that in Figure 1. The areas which are not covered by any mapolas show up as columns, the tops of which do not represent an actual value.

In Figure 3, we show the bigmap from both maplets and mapolas. This is similar to the mapola-only version, except that the mapola coverage gaps are filled in by the SPC solution.

Discussion: We see that the SPCOLA topography gives a lower RMS error (12 cm) with respect to the truth than SPC alone (34 cm). The SPCOLA error is comparable to that from OLA alone (11 cm) but fills in gaps in lidar coverage with SPC solution (although we do not anticipate any such gaps during the actual mission). The result is a combined product with higher fidelity than either data set singly. The OLA accuracy can be further improved by using the SPC solution to correct the position of individual OLA tracks.

The current SPCOLA example most closely resembles the OLA solution because we are starting with higher-resolution mapolas than maplets, and the former are given more weight. However, we could easily see the reverse situation particularly early in the mission when the OLA coverage is sparser. Thus, this combination requires some care in appropriately weighting the datasets to achieve meaningful improvement of the DEMs. The final step is to create a global shape model of Bennu from the combined maplets and mapolas.

References: [1] Gaskell, R. W., et al. (2008), *MAPS 43*, 1049-1061. [2] Roberts, J. H. (2012), *MAPS 49*, 1735-1748, [3] Craft, K. et al 2017, *LPSC 48* this volume. [4] Roberts, J.H. et al. (2014) *MAPS* 49, 1735–1748. [5] Ernst C.M. et al. (2015) *LPSC 46*, 1832. [6] Gaskell R.W. et al. (2009) *AGU Spring*, #P13A-04. [7] Jorda L. et al. (2011) *EPSC-DPS Joint Meeting*, 776. [8] Gaskell R.W. et al. (2006) *LPSC 37*, 1876. [9] Gaskell R.W. et al. (2012) *DPS*, #209.03. [10] Gaskell R.W. (2014) *DPS*, #209.04. [11] Gaskell R.W. (2011) *LPSC 42*, 1608. [12] Perry, M.E. et al. (2015) *GRL 42*, 6951–6958. [13] Weirich, J.W. et al. (2017) *LPSC 48*, this volume. [14] Perry, M.E. et al. (2017) *LPSC 48*, this volume.

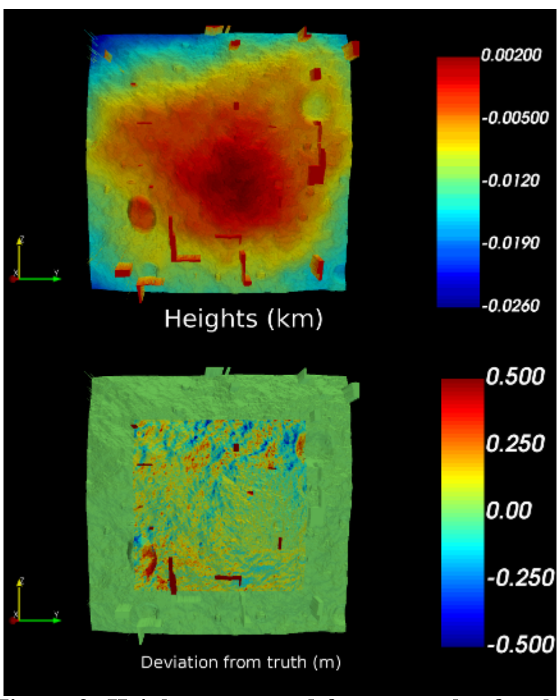

Figure 2: Heights generated from mapolas for the region shown in Figure 1 (top) and deviation from truth (bottom). The tops of the columns represent gaps between mapolas, and not real heights.

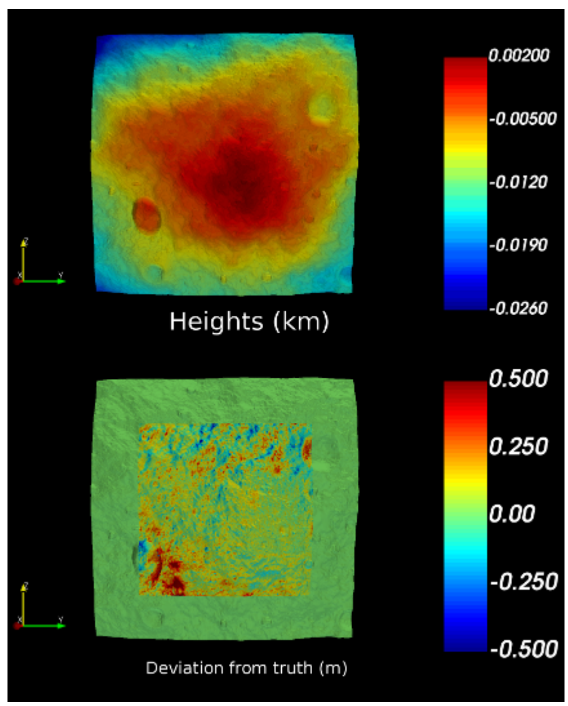

Figure 3: Heights generated from both maplets and mapolas for region shown in Figure 1 (top) and deviation from truth (bottom).